

# ASYMPTOTIC-NUMERICAL STUDY OF SUPERSENSITIVITY FOR GENERALIZED BURGERS EQUATIONS

MARC GARBEY\* AND HANS G. KAPER†

**Abstract.** This article addresses some asymptotic and numerical issues related to the solution of Burgers' equation,  $-\varepsilon u_{xx} + u_t + uu_x = 0$  on  $(-1, 1)$ , subject to the boundary conditions  $u(-1) = 1 + \delta$ ,  $u(1) = -1$ , and its generalization to two dimensions,  $-\varepsilon \Delta u + u_t + uu_x + uu_y = 0$  on  $(-1, 1) \times (-\pi, \pi)$ , subject to the boundary conditions  $u|_{x=1} = 1 + \delta$ ,  $u|_{x=-1} = -1$ , with  $2\pi$  periodicity in  $y$ . The perturbation parameters  $\delta$  and  $\varepsilon$  are arbitrarily small positive and independent; when they approach 0, they satisfy the asymptotic order relation  $\delta = O_s(e^{-a/\varepsilon})$  for some constant  $a \in (0, 1)$ .

The solutions of these convection-dominated viscous conservation laws exhibit a transition layer in the interior of the domain, whose position as  $t \rightarrow \infty$  is supersensitive to the boundary perturbation. Algorithms are presented for the computation of the position of the transition layer at steady state. The algorithms generalize to viscous conservation laws with a convex nonlinearity and are scalable in a parallel computing environment.

**AMS subject classifications.** Primary 35B25, 35B30; Secondary 35Q53, 65M55

**Key words.** Asymptotic analysis, domain decomposition, Burgers' equation, viscous conservation laws, transition layers, supersensitivity

**1. Introduction.** In this article we address some asymptotic and numerical issues related to the solution of Burgers' equation,

$$(1) \quad -\varepsilon u_{xx} + u_t + uu_x = 0 \quad \text{on } (-1, 1), \quad u(-1) = 1 + \delta, \quad u(1) = -1,$$

and its generalization to two dimensions,

$$(2) \quad \varepsilon \Delta u + u_t + uu_x + \beta uu_y = 0 \quad \text{on } (-1, 1) \times (-\pi, \pi), \quad u|_{x=-1} = 1 + \delta, \quad u|_{x=1} = -1.$$

In the latter case, we assume periodicity (period  $2\pi$ ) in the second coordinate ( $y$ ). The perturbation parameters  $\delta$  and  $\varepsilon$  are arbitrarily small positive; they are independent, but when they approach 0, they satisfy the asymptotic order relation

$$(3) \quad \delta = O_s(e^{-a/\varepsilon}) \quad \text{as } \delta, \varepsilon \downarrow 0,$$

for some constant  $a \in (0, 1)$  which does not depend on  $\delta$  or  $\varepsilon$ . This asymptotic relation implies that  $\delta$  is transcendently small (in the sense of asymptotic analysis) compared with  $\varepsilon$ , but  $\delta$  dominates  $e^{-1/\varepsilon}$  as  $\varepsilon \downarrow 0$ . (See [1, 2, 3, 4, 5] for definitions and basic concepts of asymptotic analysis.)

If  $\varepsilon = 0$ , the solution of (1) develops a shock (discontinuity) in finite time, even when the initial data are smooth [6, 7]. The perturbation introduced by a nonzero  $\varepsilon$  models the presence of viscosity, which tends to smooth the discontinuity [8, 9]. Instead of a shock, one has a transition layer—a region of rapid variation, which extends over a distance  $O(\varepsilon)$  as  $\varepsilon \downarrow 0$ . The position of the transition layer varies with time, and its eventual location at steady state is extremely sensitive to the

---

\* CDCSP-ISTIL, Université Claude Bernard Lyon 1, 69622 Villeurbanne cedex, France (garbey@cdcs.univ-lyon1.fr). Supported by the Fondation Cromeys-le-Bas under contract BS-95-2.

† Mathematics and Computer Science Division, Argonne National Laboratory, Argonne, IL 60439-4801, USA (kaper@mcs.anl.gov). Supported by the Mathematical, Information, and Computational Sciences Division subprogram of Advanced Scientific Computing Research, U.S. Department of Energy, under contract W-31-109-Eng-38.

boundary data. In fact, even the transcendently small perturbation  $\delta$  leads to a measurable (that is, order one) effect on the eventual location of the transition layer. This phenomenon, known as *supersensitivity*, was first observed by Lorentz [10]. It has been studied extensively for Burgers' equation and more general viscous conservation laws in one dimension by Kreiss and Kreiss [11], Kreiss [12], Laforgue and O'Malley [13, 14, 15, 16, 17, 18], and Reyna and Ward [19, 20, 21].

An example from combustion theory shows that supersensitivity is of more than mathematical significance. A simple model of flame propagation in gaseous fuels involves a system of two coupled convection-diffusion equations, one for the temperature of the mixture, another for the concentration of the reaction-limiting component in the mixture [22, § 3.2]. If one ignores exponentially small perturbations in the data, one finds that the Lewis number  $\mathcal{L}$ , which is a measure for the ratio of heat and mass transfer in the mixture, has no effect on the location of the combustion front. Yet, numerical computations show that this location is very sensitive—in fact, supersensitive—to the value of  $\mathcal{L}$ .

Although the phenomenon of supersensitivity is fairly well understood theoretically, at least for one-dimensional problems, the numerical solution of such problems still poses formidable challenges, especially in more than one dimension. The methods that have been proposed in the numerical literature for singularly perturbed boundary-value problems (see, for example, [23]) tend to focus on uniform approximations or finite elements with special features, not on the supersensitive dependence of the transition layer on the boundary data. On the other hand, the algorithms we propose are designed specifically to capture the phenomenon of supersensitivity. They use the fact that the solution approaches a certain profile as the perturbation parameters approach zero and focus on the computation of the corrections.

Our ultimate goal is to develop algorithms for multidimensional problems that are, first of all, suitable for long-time integration, so stable steady states can be computed with confidence; second, extremely accurate in space, so the eventual location of transition layers can be predicted with accuracy; and third, scalable in a multi-processing environment, so large-scale problems can be solved in a reasonable length of time. Although we discuss only Burgers' equation and its generalization to two dimensions, the algorithms are not restricted by the special form of the nonlinearity.

In § 2 we consider Burgers' equation. We propose a simple algorithm that effectively captures the supersensitive location of the transition layer at steady state. We stress the importance of the regions outside the transition layer, where the solution does not yet deviate appreciably from the boundary values. In § 3 we address the generalized Burgers equation in two dimensions. We show through a formal asymptotic analysis that the location of the transition layer may vary in the direction of periodicity ( $y$ ), but the transition layer is essentially flat, and only its average position (averaged over  $y$ ) depends supersensitively on the small parameters. We then develop an algorithm that effectively approximates the transition layer.

**2. One-Dimensional Case.** We begin by considering Eq. (1),

$$(4) \quad -\varepsilon u_{xx} + u_t + uu_x = 0 \quad \text{on } (-1, 1), \quad u(-1) = 1 + \delta, \quad u(1) = -1.$$

As shown by Laforgue and O'Malley [16], the solution approaches a certain profile function as  $\varepsilon \downarrow 0$ ,

$$(5) \quad u(x, t) = \tanh \eta + e^{-a/\varepsilon} u_1(\eta, \sigma) + \dots,$$

where

$$(6) \quad \eta = \frac{x - x^*(\sigma)}{\varepsilon}, \quad \sigma = te^{-a/\varepsilon}.$$

The hyperbolic tangent incorporates a transition layer centered at  $x^*$ , which connects the limiting values  $\pm 1$  at  $\mp\infty$ . Note that these limiting values are transcendently close to the prescribed boundary values  $1 + \delta$  and  $-1$  of  $u$  at  $-1$  and  $1$ . The position of the transition layer varies on a transcendently slow time scale; if  $\delta = 2be^{-a/\varepsilon}$ , its limit as  $\sigma \rightarrow \infty$  is

$$(7) \quad x_{\text{as}}^* = 1 - a + \varepsilon \ln b.$$

The important points to observe are that, first, the solution  $u$  approaches a certain profile function as  $\varepsilon \downarrow 0$ ; second, the accurate determination of the steady-state position of the transition layer requires long-term integration; and, third, a transcendently small perturbation of the boundary data has a measurable effect on the location of the transition layer.

The asymptotic analysis has been generalized to more general nonlinearities by Laforgue and O'Malley [17, 18] and Reyna and Ward [19], with similar results. One finds a limiting profile, which generalizes the hyperbolic tangent function, and a transition layer which moves on a transcendently slow time scale to a steady-state position. This position depends supersensitively on the boundary perturbation. Whenever this situation arises, appropriate variants of the following algorithms can be developed.

**2.1. Spatial Approximation.** To approximate the solution in space, we use a domain decomposition method with two non-overlapping subdomains, where the interface is located approximately at the center of the transition layer, an adaptive pseudo-spectral method on each subdomain, and collocation based on Tchebychev polynomials, where the collocation points are concentrated in the transition layer. The algorithm is standard and has been described elsewhere [24, 25, 26, 27, 28]; we summarize it here only for completeness.

Let  $x^* \in (-1, 1)$  denote the (approximate) position of the center of the transition layer;  $x^*$  varies in time ( $t$ ), but since  $t$  enters only as a parameter in the discussion of the spatial approximation, we do not write it explicitly. We decompose,

$$(8) \quad \Omega_1 = (-1, x^*), \quad \Omega_2 = (x^*, 1),$$

and map each of the subdomains  $\Omega_1$  and  $\Omega_2$  linearly onto  $(-1, 1)$ ,

$$g_1 : y \in (-1, 1) \mapsto x = g_1(y) = -1 + \frac{1}{2}(x^* + 1)(y + 1) \in \Omega_1,$$

$$g_2 : y \in (-1, 1) \mapsto x = g_2(y) = 1 - \frac{1}{2}(1 - x^*)(1 - y) \in \Omega_2.$$

The restrictions of  $u$  to  $\Omega_1$  and  $\Omega_2$  exhibit boundary layer behavior near  $x^*$ . The point  $x = x^*$  corresponds to  $y = 1$  under  $g_1$  and to  $y = -1$  under  $g_2$ . To concentrate the collocation points near  $x^*$ , we define a one-parameter family of nonlinear mappings of the interval  $(-1, 1)$  onto itself,

$$f_1(\cdot, \alpha) : s \in (-1, 1) \mapsto y = f_1(s, \alpha) = 1 - (4/\pi)\arctan(\alpha \tan \frac{1}{4}(1 - s)\pi) \in (-1, 1),$$

$$f_2(\cdot, \alpha) : s \in (-1, 1) \mapsto y = f_2(s, \alpha) = -1 + (4/\pi)\arctan(\alpha \tan \frac{1}{4}(s + 1)\pi) \in (-1, 1).$$

If the parameter  $\alpha$  is small,  $f_1$  concentrates points near 1 and  $f_2$  concentrates points near  $-1$ . Concentrating points near critical points is the computational analog of coordinate stretching in asymptotic analysis. The choice of  $\alpha$  can be optimized by means of *a priori* estimates [24, 25]; we usually take  $\alpha = \varepsilon^{1/2}$  [27]. The composite maps,

$$h_i(\cdot; \alpha) = g_i(\cdot) \circ f_i(\cdot, \alpha), \quad i = 1, 2,$$

are one-to-one from  $(-1, 1)$  onto  $\Omega_i$ ; we denote their inverses by  $h_i^{-1}(\cdot; \alpha)$ ,  $i = 1, 2$ .

We look for the solution of Eq. (4) by approximating locally on each of the subdomains  $\Omega_1$  and  $\Omega_2$  and imposing  $C^1$  continuity at  $x^*$ . If  $U$  denotes the global approximation, then

$$U(x) = U_i(x) \quad \text{for } x \in \Omega_i, \quad U \in C^1([-1, 1]).$$

The local approximations consist of finite sums of Tchebychev polynomials,

$$U_i(x) = \sum_{j=0}^{N-1} a_{ij} T_j(h_i^{-1}(x; \alpha)), \quad x \in \Omega_i, \quad i = 1, 2; \quad T_j(\cos \theta) = \cos(j\theta), \quad \theta = \pi/N.$$

**2.2. Integration for Times of Order One.** For short-time integration it suffices to combine a one-step forward Euler approximation with an implicit treatment of the second-order spatial derivative and an explicit treatment of the nonlinear term.

Starting with an approximate solution  $U^0 = U(\cdot, t_0)$  at time  $t_0$ , we identify the point  $x^* = x^*(t_0)$  with the location of the zero of  $U^0$ , partition the domain in two subdomains, and select the collocation points. Fixing this configuration temporarily, we compute a sequence  $\{U^n : n = 1, 2, \dots\}$  of successive approximations  $U^n$  using the algorithm

$$(9) \quad -\varepsilon D^2 U^n + \frac{U^n - U^{n-1}}{\Delta t} + U^{n-1} D U^{n-1} = 0, \quad n = 1, 2, \dots$$

The symbol  $D$  represents the pseudo-spectral differentiation operator in physical space [29]. The time step  $\Delta t$  is constant, so  $U^n$  is the approximate solution of the boundary-value problem (1) at  $t_0 + n\Delta t$ . The algorithm (9) is nonconservative.

When the location of the zero of  $U^n$  has moved over a distance  $\varepsilon$ , we suspend the algorithm (9). We shift  $x^*$  to the current location of the zero, reconfigure the partition, update the collocation points, replace  $U^0$  by the values at the new collocation points (using interpolation if necessary), and continue the algorithm (9). We repeat this process until the steady state is reached. The change in the location of the zero of the computed approximation becomes smaller as time progresses, so the same collocation configuration serves for longer and longer time intervals.

The algorithm (9) requires the solution of  $U^n$  from the equation

$$(10) \quad A U^n = U^{n-1} + (\Delta t) U^{n-1} D U^{n-1}.$$

The matrix  $A$ , which is order  $2N - 1$ , has a block structure,

$$A = \begin{pmatrix} A_1 & b_1 & \\ a_1^t & c & b_2^t \\ & a_2 & A_2 \end{pmatrix}.$$

$A_1$  and  $A_2$  are square matrices of order  $N - 1$ ;  $a_1$ ,  $a_2$ ,  $b_1$ , and  $b_2$  vectors of length  $N - 1$ ;  $c$  is a constant. The center row accounts for the  $C^1$  continuity at the interface. This block structure allows a solution of the system (10) in two parallel processes from opposite ends. The matrix  $A$  does not change as long as the collocation configuration is frozen. However, its condition number increases with the number of collocation points. This increase puts a lower limit on the values of  $\delta$  one can handle in practice.

TABLE 1  
*Location of the transition layer at steady state.*

$\delta$	$\varepsilon = 0.1$		$\varepsilon = 0.05$	
	$x_\infty^*$	$x_{as}^*$	$x_\infty^*$	$x_{as}^*$
$1.0 \cdot 10^{-1}$	0.72464	0.700427	0.86237	0.850213
$1.0 \cdot 10^{-2}$	0.47486	0.470176	0.73755	0.735084
$1.0 \cdot 10^{-3}$	0.24133	0.240724	0.62055	0.619955
$1.0 \cdot 10^{-4}$	0.05265	0.052606	0.50485	0.504826
$1.0 \cdot 10^{-5}$	0.00537	0.005504	0.38962	0.389696

Table 1 gives the location of the transition layer at steady state,  $x_\infty^*$ , computed with the algorithm (9) with  $N = 39$  collocation points in each subdomain and a time step  $\Delta t = 0.02$ . The number  $x_{as}^* = 1 - \varepsilon \ln(2/\delta)$ , which is an asymptotic estimate of  $x^*$  (see Eq. (7)) is given for comparison. The initial conditions were usually obtained by linear interpolation from the boundary data, but variations were made to test the answers. The lower limit on  $\varepsilon$  is determined by the fact that the computation time for the algorithm (9) increases as  $\varepsilon$  decreases. In § 2.4 we discuss an algorithm suitable for long-time integration.

Table 2 shows the impact of grid refinement (the number of collocation points,  $N$ ) on the value of  $x_\infty^*$ .

TABLE 2  
*Effect of grid refinement ( $N$ ) on  $x_\infty^*$ ;  $\varepsilon = 0.1$ ,  $\delta = 1.0 \cdot 10^{-3}$ .*

$N$	15	19	29	39	49	59
$x_\infty^*$	0.25576	0.24115	0.24166	0.24133	0.24140	0.24143

**2.3. Neglecting Viscosity.** In supersensitive boundary-value problems, the solution in the “tails” on either side of the transition layer is exponentially close to the prescribed boundary values, so the viscous term is exponentially small there. It is therefore tempting to assume that one can sacrifice some accuracy in the computation of the viscous term during the transient phase and still find the position of the transition layer at steady state with a high degree of accuracy.

An extreme form of this assumption underlies the approach where one constructs a first approximation by ignoring the viscous term altogether. Using a conservative finite-difference scheme, such as Godunov, one constructs the entropy solution of the inviscid conservation law ( $\varepsilon = 0$ ) and takes this as a first approximation. One then constructs higher-order uniform approximations, for example by means of a heterogeneous domain-decomposition method, using either a different numerical scheme to solve the full viscid problem in the interior of the transition layer or some other approximation of the viscous equation.

The  $\chi$  method introduced by Brezzi et al. [30] is a more sophisticated nonlinear adaptive scheme based on the same assumption. Here, one replaces the boundary-

value problem by

$$(11) \quad -\varepsilon\chi(u_{xx}) + u_t + (f(u))_x = 0 \text{ on } (-1, 1), \quad u(-1, t) = 1 + \delta, \quad u(1, t) = -1,$$

where  $\chi \equiv \chi_{\sigma, \tau}$  is a smooth monotone function,  $\chi(s) = 0$  if  $|s| \leq \sigma$  and  $\chi(s) = s$  if  $|s| \geq \sigma + \tau$  for some positive numbers  $\sigma$  and  $\tau$ . This method has been applied to Burgers' equation [31] and the incompressible Navier-Stokes equations [32]. However, we claim that the  $\chi$  method cannot accurately predict the ultimate position of the transition layer, at least for Burgers' equation on a finite interval with Dirichlet data. This claim is supported by the following observations.

Consider the results quoted in [31, Table II]. With few exceptions, they involve relatively large values of  $\sigma$  ( $\sigma$  is called  $\delta$  in [31]); in fact,  $\sigma$  is typically greater than  $\varepsilon^{-1/2}$  ( $\varepsilon$  is called  $\nu$  in [31]) by one or two orders of magnitude. The viscous term is therefore always neglected, unless  $u_{xx}$  is of the same order as  $\varepsilon^{-1/2}$ ; that is, the viscous term is neglected everywhere except in the transition layer. If the  $\chi$  method gave the correct position of the transition layer at steady state, then the same would certainly be the case when we simply multiply the viscous term by a smooth function of position, whose support is of order one and includes the transition layer. After all, in the latter case we account for the viscous term over a much broader region. These arguments lead us to consider the boundary-value problem

$$(12) \quad -\varepsilon H(x)u_{xx} + u_t + uu_x = 0 \text{ on } (-1, 1), \quad u(-1, t) = 1 + \delta, \quad u(1, t) = -1,$$

instead of the boundary-value problem (11). Here,  $H$  is a smooth cut-off function,

$$(13) \quad H(x) = \begin{cases} \frac{1}{2}(1 - \tanh(\alpha(x - x^*(t) + \beta))), & x < x^*(t), \\ \frac{1}{2}(1 + \tanh(\alpha(-x + x^*(t) + \beta))), & x > x^*(t). \end{cases}$$

We use a numerical approximation of  $x^*(t)$  and choose the parameters  $\alpha$  and  $\beta$  so

$$H(x) = 1 \text{ if } |x - x^*(t)| < \frac{1}{2}\beta, \quad H(x) = 0 \text{ if } |x - x^*(t)| > \frac{3}{2}\beta,$$

to within machine accuracy ( $1 \cdot 10^{-15}$ ). The algorithm (9) leads to the solution of  $U^n$  from the equation

$$(14) \quad -\varepsilon H D^2 U^n + \frac{U^n - U^{n-1}}{\Delta t} + U^{n-1} D U^{n-1} = 0, \quad n = 1, 2, \dots$$

The results given in Table 3 (computed for  $\varepsilon = 0.1$  and  $\delta = 1.0 \cdot 10^{-2}$ , with  $\alpha = 200$ ) show that the algorithm (14) can give incorrect results for the position of the transition layer at steady state. (The correct value is  $x_\infty^* = 0.47486$ , see Table 1.) The position

TABLE 3  
*Location of the transition layer at steady state computed with the  $\chi$  method.*

$\beta$	0.1	0.2	0.3	0.4	0.5	0.6	0.7
$x_\infty^*$	0.0056	0.0110	0.0174	0.0384	0.0923	0.1067	0.1565

of the shock freezes too early during the transient phase. The actual moment of freezing depends on the size of the zone to the left of the transition layer (where  $H \equiv 0$ ). The result improves as  $\beta$  increases, but for  $\beta = 0.8$  the algorithm fails to converge. (The position of the transition layer keeps oscillating between the regions

where  $H \equiv 1$  and  $H \equiv 0$ .) On the other hand, if we include the missing part of the viscous term explicitly and use the algorithm

$$(15) \quad \varepsilon H D^2 U^n - \varepsilon (1 - H) D^2 U^{n-1} + \frac{U^n - U^{n-1}}{\Delta t} + U^{n-1} D u^{n-1} = 0, \quad n = 1, 2, \dots,$$

instead of (14), we retrieve the correct position of the transition layer at steady state. This result demonstrates clearly that, when the problem is supersensitive, it is not advisable to neglect the viscous term, even when that term is exponentially small.

Note that the modified algorithm (15) treats the second-order derivative explicitly in the region where  $H \equiv 0$  and implicitly in the region where  $H \equiv 1$ . The idea of using a cutoff function to construct a composite algorithm is described in detail in our article [28]. The procedure offers a very general tool for the design of heterogeneous domain decompositions in the framework of a finite-difference approximation. However, since the algorithm (15) is based on a Tchebyshev pseudo-spectral approximation, the partially explicit treatment of the viscous term forces a severe constraint on the time step that cannot be circumvented. For example, with  $\varepsilon = 0.1$  and  $N = 49$  collocation points per subdomain, the time step must be 10 times smaller than the time step for the algorithm (9). The algorithm (15) is therefore certainly not practical for long-time integration.

**2.4. Long-Time Integration.** The explicit treatment of the nonlinear term in the algorithm (9) imposes a severe constraint on the time step (CFL condition). The algorithm is therefore not suitable for long-time integration. The alternative approach commonly taken is to use a fully implicit scheme in combination with a Newton algorithm [33]. However, an implicit scheme can be expensive and is certain to increase interprocessor communication in a multiprocessing environment. If the solution of the viscous conservation law is close to a certain profile function, as is the case for Burgers' equation, at least after an initial transient, the following algorithm offers a more efficient alternative.

We start the integration of Eq. (4) at  $t = t_0$ , say, when we have an approximate profile with a transition layer centered at  $x^*$ . We construct the function  $u_0$ ,

$$(16) \quad u_0(x) = -\tanh \frac{x - x^*}{2\varepsilon},$$

which satisfies Burgers' equation exactly, and look for a solution  $u$  of the form

$$(17) \quad u(x, t) = u_0(x) + \delta v(x, t).$$

Then  $v$  must satisfy the nonlinear boundary-value problem

$$-\varepsilon v_{xx} + v_t + u_0 v_x + u_0' v + \delta v v_x = 0 \quad \text{on } (-1, 1),$$

$$v(-1, t) = \delta^{-1}(1 + \delta - u_0(-1)), \quad v(1, t) = \delta^{-1}(-1 - u_0(1)).$$

We integrate this boundary-value problem for  $t > t_0$ , using the algorithm

$$(18) \quad \varepsilon D^2 V^n + \frac{V^n - V^{n-1}}{\Delta t} + u_0 D V^n + u_0' V^n = -\delta V^{n-1} D V^{n-1}, \quad n = 1, 2, \dots,$$

and define an approximation  $U$  of  $u$  for  $t > t_0$ ,

$$(19) \quad U(x, t) = u_0(x) + \delta V(x, t), \quad t > t_0.$$

We proceed with the integration as long as the supremum of  $U(\cdot, t) - u_0$  remains of the order of  $\delta$ . When this criterion is no longer met, at  $t = t_1$  say, we suspend the integration, identify the point  $x^*$  with the location of the center of the transition layer at  $t_1$ , update the profile function  $u_0$ , and continue the integration beyond  $t_1$ . We repeat the procedure until the steady state is reached. Figure 1 shows a profile function  $u_0$  and the computed solution  $U(\cdot, t)$  at some time  $t$ . Note that the former is monotone, the latter is not.

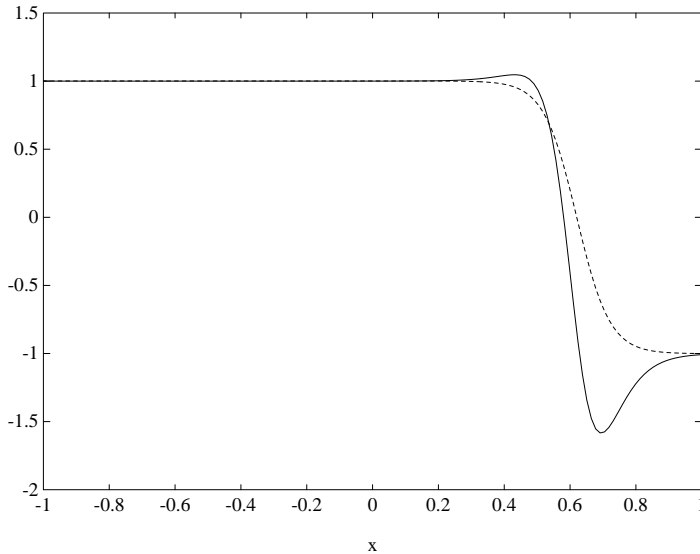


FIG. 1. The profile function  $u_0$  (dashed line) and the computed solution  $U(\cdot, t)$  at some time  $t$  (solid line);  $\varepsilon = 0.05$ ,  $\delta = 1 \cdot 10^{-3}$ .

The algorithm (18) is very similar to (9). The spatial approximation is handled with the same domain-decomposition method, so the structure of the resulting linear system is the same as in Eq. (10). But the constraint on the time step is relaxed by a factor  $\delta$ . With the algorithm (18) we can integrate the boundary-value problem for values of  $\varepsilon$  as small as 0.01, down to  $\delta$ s of the order of  $10^{-6}$ , using time steps that are typically 50 times larger than with the algorithm (9). Table 4 gives some results for  $x_\infty^*$ , computed with the algorithm (18), with  $N = 39$  collocation points in each subdomain.

TABLE 4  
Location of the transition layer at steady state.

	$\varepsilon = 0.1$	$\varepsilon = 0.05$	$\varepsilon = 0.02$	$\varepsilon = 0.01$
$\delta$	$x_\infty^*$	$x_\infty^*$	$x_\infty^*$	$x_\infty^*$
$1.0 \cdot 10^{-1}$	0.72346	0.86175		
$1.0 \cdot 10^{-2}$	0.47508	0.73774	0.89518	
$1.0 \cdot 10^{-3}$	0.24140	0.62057	0.84827	0.92429
$1.0 \cdot 10^{-4}$	0.05275	0.50485	0.80210	0.90104
$1.0 \cdot 10^{-5}$	0.00561	0.38964	0.75609	0.87800
$1.0 \cdot 10^{-6}$	0.00066	0.27452	0.70996	0.85482
$1.0 \cdot 10^{-7}$				0.83084

**3. Two-Dimensional Case.** Next, we consider Burgers' equation generalized to two dimensions,

$$(20) \quad \Delta u + u_t + uu_x + \beta uu_y = 0 \quad \text{on } (-1, 1) \times (-\pi, \pi), \quad u|_{x=-1} = 1 + \delta, \quad u|_{x=1} = -1.$$

We assume periodicity in  $y$  (period  $2\pi$ ). The perturbation  $\delta$  may vary with  $y$ ; its Fourier expansion is

$$(21) \quad \delta \equiv \delta(y) = \delta_0 \sum_{k \in \mathbf{Z}} \eta_k e^{iky}.$$

The coefficients  $\eta_k$ , as well as the pre-factor  $\delta_0$ , are independent of  $y$ . The pre-factor  $\delta_0$  is arbitrarily small positive and defined in such a way that  $\eta_0 = 1$  and  $\eta_k = O(1)$  as  $\delta_0 \downarrow 0$  for  $k = \pm 1, \pm 2, \dots$ . The order relation (3) between  $\delta$  and  $\varepsilon$ , which must hold uniformly in  $y$ , implies that

$$(22) \quad \delta_0 = O_s(e^{-a/\varepsilon}) \quad \text{as } \delta_0, \varepsilon \downarrow 0,$$

for some  $a \in (0, 1)$ . We show in § 3.1 that, under these conditions, the *average* position of the transition layer (averaged over  $y$ ) depends supersensitively on the small parameters  $\varepsilon$  and  $\delta_0$ . In § 3.2 we briefly review the spatial approximation. § 3.3 is devoted to the integration procedure.

**3.1. Profile Function.** The algorithm we propose for the solution of the boundary-value problem (20) is again based on the assumption that the solution is close to a known profile function. Our goal in this section is to show that, under the conditions given above, the profile function is asymptotically independent of  $y$  and again given to leading order by the hyperbolic tangent, as in Eq. (5).

We introduce the constant  $x^* \in (0, 1)$  such that  $x^* \sim 1 - \varepsilon \ln(2/\delta_0)$  as  $\varepsilon \downarrow 0$ . We define the function  $u_0$ ,

$$(23) \quad u_0(x) = -\tanh \frac{x - x^*}{2\varepsilon},$$

and look for a profile function  $\varphi$  of the form

$$(24) \quad \varphi(x, y) = u_0(x) + v(x, y).$$

Because  $u_0$  satisfies Burgers' equation,  $v$  must satisfy the differential equation

$$(25) \quad -\varepsilon \Delta v + u_0 v_x + u_0' v + \beta u_0 v_y + v v_x + \beta v v_y = 0,$$

together with the boundary conditions

$$(26) \quad v|_{x=-1} = \delta - \delta_0, \quad v|_{x=1} = 0.$$

The linearized equation,

$$(27) \quad \ell(v) \equiv -\varepsilon \Delta v + u_0 v_x + u_0' v + \beta u_0 v_y = 0,$$

has a solution,  $\ell(u_0') = 0$ , so we reduce the order by substituting

$$(28) \quad v = u_0' w.$$

Then  $w$  must satisfy the equation

$$(29) \quad -\varepsilon \Delta w - u_0 w_x + \beta u_0 w_y = 0,$$

together with the boundary conditions

$$(30) \quad w|_{x=-1} = (\delta - \delta_0)/u_0'(-1), \quad w|_{x=1} = 0.$$

We estimate  $w$  by means of the coefficients in its Fourier expansion,

$$(31) \quad w(x, y) = \sum_{k \in \mathbf{Z}} w_k(x) e^{iky}.$$

The leading coefficient  $w_0$  is the solution of the boundary-value problem

$$(32) \quad -\varepsilon w_0'' - u_0 w_0' = 0 \quad \text{on } (-1, 1), \quad w_0(-1) = 0, \quad w_0(1) = 0.$$

so  $w_0 = 0$ . Note that this result is a direct consequence of the fact that we have defined  $x^*$  in terms of the average  $\delta_0$  in Eq. (23); any other definition leads to an inhomogeneous boundary-value problem, whose solution  $w_0$  does not vanish.

The remaining coefficients  $w_k$ ,  $k = \pm 1, \pm 2, \dots$ , are found from the boundary-value problem

$$(33) \quad -\varepsilon w_k'' - u_0 w_k' + (\varepsilon k^2 + i\beta k u_0) w_k = 0, \quad w_k(-1) = \delta_0 \eta_k, \quad w_k(1) = 0.$$

This is a classical turning-point problem, as  $u_0$  changes sign in the interval  $(-1, 1)$ . The asymptotic behavior of  $w_k$  as  $\varepsilon \downarrow 0$  can be found by the method described in [3, § 3.E],

$$(34) \quad w_k(x) \sim \left[ c_k e^{i\beta k x} + (1 - c_k e^{-i\beta k}) e^{-(1+x)/\varepsilon} + (0 - c_k e^{i\beta k}) e^{-(1-x)/\varepsilon} \right] w_k(-1).$$

The coefficient  $c_k$  is such that the functional

$$(35) \quad \mathcal{L}[w] = \frac{1}{2} \int_{-1}^1 [\varepsilon w'^2 + (\varepsilon k^2 + i\beta k u_0) w^2] \exp\left(\frac{1}{\varepsilon} \int_0^x u_0(\xi) d\xi\right) dx$$

has a critical point at  $w = w_k$ ,

$$(36) \quad \frac{\partial \mathcal{L}[w_k]}{\partial c_k} = 0.$$

Notice that the differential equation (33) is the Euler equation of the functional  $\mathcal{L}$ ; the Neumann boundary conditions  $w_k'(\pm 1) = 0$  are the natural boundary conditions associated with  $\mathcal{L}$ .

Obviously, finding an explicit expression for  $c_k$  is out of the question. The best we can aim for is an asymptotic expansion as  $\varepsilon \downarrow 0$ , and even here we must resort to computational assistance. Using the symbolic manipulation language MAPLE, we find

$$(37) \quad c_k \sim \frac{e^{-(x^*+1)/\varepsilon}}{(1 + \beta^2)\varepsilon^2 k^2} e^{-i\beta k(1+2x^*)} \quad \text{as } \varepsilon \downarrow 0.$$

The first term in the brackets in Eq. (34) represents the regular part of the asymptotic behavior of  $w_k$ , which dominates in the interior; the remaining two terms represent

the singular part, which dominates near the endpoints of the interval. Since we are interested in the transition layer, which is located in the interior, we ignore the singular part and take only the regular part,  $w_k(x) \sim c_k w_k(-1) e^{i\beta k x}$ . That is, we take

$$(38) \quad v_k(x) \sim \frac{\delta_0 \eta_k e^{-(1+x^*)/\varepsilon}}{(1+\beta^2)\varepsilon^2 k^2} \frac{u'_0(x)}{u'_0(-1)} e^{i\beta k(1-2x^*+x)} \quad \text{as } \varepsilon \downarrow 0.$$

If we use the asymptotic approximation

$$\frac{u'_0(x)}{u'_0(-1)} = \frac{1 - \tanh^2((x-x^*)/(2\varepsilon))}{1 - \tanh^2((-1-x^*)/(2\varepsilon))} \sim \frac{1 - \tanh^2((x-x^*)/(2\varepsilon))}{4e^{-(1+x^*)/\varepsilon}},$$

we obtain the asymptotic expression

$$(39) \quad v_k(x) \sim \frac{\delta_0 \eta_k}{4(1+\beta^2)\varepsilon^2 k^2} e^{i\beta k(1-2x^*+x)} \left( 1 - \tanh^2 \frac{x-x^*}{2\varepsilon} \right).$$

This result implies that the Fourier series of  $v$ , as well as those of  $v_x$  and  $v_y$ , converge. Furthermore,  $\|v\|_\infty$  and  $\|v_y\|_\infty$  are  $O(\delta_0 \varepsilon^{-2})$ .

Finding the asymptotic behavior of  $\|v_x\|_\infty$  is less obvious. It follows from Eq. (34) that  $w'_k(x) \sim c_k e^{i\beta k x}$  as  $\varepsilon \downarrow 0$ , at least for  $x$  in the interior of the domain. Therefore,  $v'_k(x) = (u'_0 w_k)'(x) \sim (u''_0 w_k)(x) \sim \varepsilon^{-1} (u'_0 w_k)(x) = \varepsilon^{-1} v_k(x)$ . Hence,  $\|v_x\|_\infty = O(\delta_0 \varepsilon^{-3})$  as  $\delta_0, \varepsilon \downarrow 0$ .

Since  $\delta_0 = O_s(e^{-a/\varepsilon})$  for some  $a \in (0, 1)$ , we have  $\delta_0 \varepsilon^{-p} = O_s(e^{-a'/\varepsilon})$  ( $p = 2, 3$ ) for any  $a' \in (0, a)$ , so any solution  $v$  of Eq. (27) which satisfies the boundary conditions (26) is transcendentally small. The residue  $vv_x + \beta vv_y$ , which was ignored in the transition from the nonlinear equation (25) to the linear equation (27) is likewise transcendentally small and, in fact,  $O(\delta_0^2 \varepsilon^{-5})$ , so we also have an a posteriori justification for the linearization.

These arguments motivate the choice of  $u_0$ , which depends only on  $x$ , as the profile function in the design of the numerical algorithms for Eq. (20).

**3.2. Spatial Approximation.** The spatial approximation is again based on a domain decomposition with two non-overlapping subdomains on either side of the  $y$ -averaged location of the center of the transition layer. On each subdomain we use an adaptive pseudo-spectral method in the  $x$  direction and a finite-difference method in the  $y$  direction. The pseudo-spectral method is the same as in the one-dimensional case; it uses Tchebychev polynomial collocation with  $N_x$  collocation points.

Since the transition layer is close to a plane parallel to the  $x$  axis, there is no need to resort to an adaptive grid in the  $y$  direction. For our numerical experiments we chose a regular grid with mesh width  $h = 2\pi/N_y$  and a sixth-order central finite-difference approximation of  $u_{yy}$  and  $u_y$ . The choice may seem inconsistent with the spectral approximation in the  $x$  direction; a more obvious choice would be a Fourier approximation in the  $y$  direction. Theoretically, the finite-difference approximation in the  $y$  direction restricts the accuracy of the approximation for a regular problem ( $\varepsilon = O_s(1)$ ) to sixth order, less than the accuracy guaranteed by the pseudo-spectral approximation in the  $x$  direction. However, as the transition layer is close to a plane parallel to the  $x$  axis, it is relatively easy to keep the numerical error in the finite-difference approximation of the term  $\varepsilon u_{yy}$  smaller than the numerical error in the pseudo-spectral approximation of the term  $\varepsilon u_{xx}$  with a moderate number of discretization points  $N_y$ . There is, therefore, no need to use a better approximation, like

the Fourier approximation, for the term  $\varepsilon u_{yy}$ . Furthermore, the spectral radius of  $D_y^2$  is smaller with sixth-order finite differences than with Fourier differentiation. This difference implies an additional advantage for a finite-difference approximation when the  $y$  derivatives are treated explicitly [34].

**3.3. Integration for Times of Order One.** We extend the Euler scheme (9) to two dimensions as follows:

$$-\varepsilon D_x^2 U^n + \frac{U^n - U^{n-1}}{\Delta t} = \varepsilon D_y^2 U^{n-1} + U^{n-1} D_x U^{n-1} + \beta U^{n-1} D_y U^{n-1}, \quad n = 1, 2, \dots \quad (40)$$

Here,  $D_x$  is the pseudo-spectral differential operator with Tchebychev polynomials,  $D_y$  the finite-difference operator with sixth-order central finite differences.

The algorithm (40) has several features that make it readily parallelizable. First, the approximations  $D_y U^{n-1}$  and  $D_y^2 U^{n-1}$  are taken explicitly, so the variable  $y$  is only a parameter. Second, because we are using finite-difference approximations, we have only local data dependencies. This latter point especially offers a significant advantage over a spectral method, which uses global interpolation.

Table 5 shows the results for the boundary-value problem (20) with  $\beta = 1$ ,  $\varepsilon = 0.1$  and piecewise constant boundary data with  $\delta_0 = 1.0 \cdot 10^{-2}$ ,

$$u(-1, y) = \begin{cases} 1.01 - \Delta\delta & \text{if } -\pi \leq y < -\frac{1}{2}\pi, \\ 1.01 + \Delta\delta & \text{if } -\frac{1}{2}\pi \leq y < \frac{1}{2}\pi, \\ 1.01 - \Delta\delta & \text{if } \frac{1}{2}\pi \leq y < \pi. \end{cases} \quad (41)$$

The algorithm (40) was applied with  $N_x = 39$  collocation points per subdomain in the  $x$  direction and  $N_y = 32$  interpolation points in the  $y$  direction. The table gives the  $y$ -averaged location of the transition layer at steady state,  $\langle x_\infty^* \rangle$ , as well as the maximum deviation of the center of the transition layer from its  $y$ -averaged location,  $\Delta x^*$ ; that is,  $x_\infty^*(y)$  varies between  $\langle x_\infty^* \rangle - \Delta x^*$  and  $\langle x_\infty^* \rangle + \Delta x^*$ . These results

TABLE 5  
Location of the transition layer at steady state; boundary data (41).

$\Delta\delta$	$\langle x_\infty^* \rangle$	$\Delta x^*$
$0.25 \cdot 10^{-2}$	0.4758	$1.3114 \cdot 10^{-2}$
$0.50 \cdot 10^{-2}$	0.4759	$2.3584 \cdot 10^{-2}$
$1.0 \cdot 10^{-2}$	0.4758	$4.8865 \cdot 10^{-2}$
$1.5 \cdot 10^{-2}$	0.4750	$7.8632 \cdot 10^{-2}$
$2.0 \cdot 10^{-2}$	0.4738	$9.3250 \cdot 10^{-2}$
$3.0 \cdot 10^{-2}$	0.4700	$15.688 \cdot 10^{-2}$

show that the algorithm (40) is extremely effective for the boundary-value problem. As  $\Delta\delta$  increases,  $\Delta x^*$  grows approximately linearly with  $\Delta\delta$ . The graph of  $U - u_0$  maintains its overall shape, so its width (which measures  $\Delta x^*$ ) varies in proportion to its height (which measures  $\|U - u_0\|_\infty$ ). The numerical results therefore indicate also that  $\|U - u_0\|_\infty$  grows approximately linearly with  $\Delta\delta$ . This conclusion matches the results of the asymptotic analysis in § 3.1, in particular Eq. (39), where it was shown that  $v_k$  is proportional to  $\eta_k$ .

Results for a much harder case are presented in Table 6. The parameters  $\beta$  and  $\varepsilon$  are fixed as before,  $\beta = 1$  and  $\varepsilon = 0.1$ , but this time the data at the left boundary are sharply peaked at the midpoint,

$$u(-1, y) = 1.005 + (\Delta\delta)e^{-20(1-\cos y)}, \quad -\pi < y < \pi. \quad (42)$$

The algorithm (40) was again applied with  $N_x = 39$  collocation points per subdomain in the  $x$  direction and  $N_y = 32$  interpolation points in the  $y$  direction. The table gives, in addition to the values of  $\langle x_\infty^* \rangle$  and  $\Delta x^*$ , the asymptotic value  $x_{as}^* = 1 - \varepsilon \ln(2/\delta_0)$ . The average location of the transition layer is predicted very well by the asymptotics.

TABLE 6  
Location of the transition layer at steady state; boundary data (42).

$\Delta\delta$	$\langle x_\infty^* \rangle$	$x_{as}^*$	$\Delta x^*$
$0.25 \cdot 10^{-2}$	0.40808	0.40811	$0.27278 \cdot 10^{-2}$
$0.50 \cdot 10^{-2}$	0.41277	0.41241	$0.37231 \cdot 10^{-2}$
$1.0 \cdot 10^{-2}$	0.42096	0.42052	$0.92263 \cdot 10^{-2}$
$2.0 \cdot 10^{-2}$	0.43573	0.43506	$1.4589 \cdot 10^{-2}$
$3.0 \cdot 10^{-2}$	0.44854	0.44782	$2.3924 \cdot 10^{-2}$

Again, the maximum deviation  $\Delta x^*$  grows with  $\Delta\delta$ , although not linearly as in the case of the step boundary data (41).

Table 7 shows the impact of grid refinement (the number of collocation points per subdomain,  $N_x$ , and the number of discretization points,  $N_y$ ) on the computed value of  $x_\infty^*(y)$  for the problem with boundary data (41),  $\Delta\delta = 0.01$ .

TABLE 7  
Effect of grid refinement ( $N_x, N_y$ ) on  $\langle x_\infty^* \rangle$  (upper entries) and  $\Delta x^*$  (lower entries); boundary data (41) with  $\Delta\delta = 0.01$ .

$N_y$	$N_x = 19$	$N_x = 29$	$N_x = 39$	$N_x = 49$	$N_x = 59$
8	0.47848	0.47653	0.47523	0.47557	0.47547
	$4.7396 \cdot 10^{-2}$	$4.8375 \cdot 10^{-2}$	$4.8902 \cdot 10^{-2}$	$5.2615 \cdot 10^{-2}$	$5.2251 \cdot 10^{-2}$
16	0.47807	0.47614	0.47610	0.47478	0.47516
	$4.7396 \cdot 10^{-2}$	$5.8062 \cdot 10^{-2}$	$4.8849 \cdot 10^{-2}$	$4.9273 \cdot 10^{-2}$	$4.9518 \cdot 10^{-2}$
32	0.47883	0.47611	0.47578	0.47536	0.47481
	$4.7396 \cdot 10^{-2}$	$4.8374 \cdot 10^{-2}$	$4.8864 \cdot 10^{-2}$	$4.9267 \cdot 10^{-2}$	$4.9516 \cdot 10^{-2}$
64	0.47847	0.47610	0.47561	0.47513	0.47524
	$4.7396 \cdot 10^{-2}$	$4.8372 \cdot 10^{-2}$	$4.8867 \cdot 10^{-2}$	$4.9266 \cdot 10^{-2}$	$5.2280 \cdot 10^{-2}$

An obvious way to parallelize the algorithm (40) is to partition the interval  $(-\pi, \pi)$  into subintervals of equal length  $2\pi/N_y$  and map this partition onto a ring of processors. Thus, one can achieve high speedups on a Paragon using nonblocking communications. If each processor covers at least four mesh points in the  $y$  direction, only nearest-neighbor communication is needed. Table 8 gives ample evidence that the algorithm (40) is highly scalable; doubling the number of processors with the problem size results in almost identical CPU times.

TABLE 8  
CPU time for 1,000 time steps on the Paragon XP/S as a function of the number of processors ( $P$ ) and the size of the problem (measured by  $N_y$ );  $N_x = 49$ .

$N_y$	$P = 1$	$P = 2$	$P = 4$	$P = 8$	$P = 16$
32	129.16	65.88	33.91	17.43	
64	252.85	130.02	65.85	33.85	17.45
128	519.05	257.85	129.68	65.85	33.92
256		515.01	257.49	129.77	65.93

Additional parallelism can be introduced by decomposing the domain in the  $x$  direction. However, our experience with a similar algorithm for combustion problems

indicates a potentially significant decrease (as much as 70%) in the efficiency of the algorithm [35].

In general, the algorithm (40) is very well adapted to the quasi one-dimensional structure of the transition layer. The algorithm predicts the location of the transition layer at steady state with a significant accuracy. The time step is of the same order of magnitude as for the one-dimensional analog (9).

**3.4. Long-Time Integration.** The algorithm (40) needs to be modified for long-time integration. We distinguish between the cases  $\beta = 0$  and  $\beta \neq 0$ .

If  $\beta = 0$ , we use an algorithm similar to the one described in § 2.4. We start the integration of Eq. (20) at  $t = t_0$ , say. We identify the point  $x^*$  with the location of the zero of the approximation  $U$  of  $u$ , averaged over  $y$ , at  $t = t_0$  and define the profile function  $u_0$  as in Eq. (23),

$$(43) \quad u_0(x) = -\tanh \frac{x - x^*}{2\varepsilon},$$

Then we integrate the nonlinear boundary-value problem

$$-\varepsilon \Delta v + v_t + u_0 v_x + u_0' v + \delta_0 \varepsilon^{-2} v v_x = 0 \quad \text{on } (-1, 1) \times (-\pi, \pi)$$

forward in time, subject to the boundary conditions

$$v|_{x=-1} = \delta_0^{-1} \varepsilon^2 (1 + \delta - u_0(-1)), \quad v|_{x=1} = \delta_0^{-1} \varepsilon^2 (-1 - u_0(1)),$$

using the algorithm

$$(44) \quad \varepsilon D_x^2 V^n + \frac{V^n - V^{n-1}}{\Delta t} + u_0 D_x V^n + u_0' V^n = \varepsilon D_y^2 V^{n-1} - \delta_0 \varepsilon^{-2} V^{n-1} D_x V^{n-1},$$

for  $n = 1, 2, \dots$ . We define the approximation  $U$  of  $u$ ,

$$(45) \quad U(x, y, t) = u_0(x) + \delta_0 \varepsilon^{-2} V(x, y, t),$$

and integrate as long as the supremum of  $U(\cdot, \cdot, t) - u_0$  remains of the order of  $\delta_0 \varepsilon^{-2}$ . When this criterion is no longer met, at  $t = t_1$  say, we suspend the integration, identify the point  $x^*$  with the location of the center of the transition layer (averaged over  $y$ ), and update the profile function  $u_0$ . We repeat the procedure until the steady state is reached.

The time step for the algorithm (44) is limited by the (explicit) term  $\varepsilon D_y^2 V^{n-1}$ ,  $\Delta t < c(2\pi/N_y)^2/\varepsilon$ , for some constant  $c < \frac{1}{2}$ . This limitation is not too severe, as  $\varepsilon$  is very small and the variation of the solution in the  $y$  direction is exponentially small, so  $N_y$  need not be large.

If  $\beta \neq 0$ , the situation becomes more complicated. One can, of course, extend the algorithm (44) trivially by incorporating the convective term in the right member,

$$(46) \quad \begin{aligned} & -\varepsilon D_x^2 V^n + \frac{V^n - V^{n-1}}{\Delta t} + u_0 D_x V^n + u_0' V^n \\ & = \varepsilon D_y^2 V^{n-1} - \delta_0 \varepsilon^{-2} V^{n-1} D_x V^{n-1} - \beta u_0 D_y V^{n-1} - \beta \delta_0 \varepsilon^{-2} V^{n-1} D_y V^{n-1}, \end{aligned}$$

for  $n = 1, 2, \dots$ . Representative results obtained in this way for the boundary-value problem (20) with  $\beta = 1$  and  $\varepsilon = 0.02$  are given in Table 9. The boundary data are again piecewise constant, as in Table 5, but with  $\delta_0 = 1.0 \cdot 10^{-6}$ ,

$$(47) \quad u(-1, y) = \begin{cases} 1 + 1.0 \cdot 10^{-6} - \Delta\delta & \text{if } -\pi \leq y < -\frac{1}{2}\pi, \\ 1 + 1.0 \cdot 10^{-6} + \Delta\delta & \text{if } -\frac{1}{2}\pi \leq y < \frac{1}{2}\pi, \\ 1 + 1.0 \cdot 10^{-6} - \Delta\delta & \text{if } \frac{1}{2}\pi \leq y < \pi. \end{cases}$$

The algorithm (46) was applied with  $N_x = 39$  collocation points per subdomain in the  $x$  direction and only  $N_y = 16$  interpolation points in the  $y$  direction. We observe

TABLE 9  
Location of the transition layer at steady state; boundary data (47).

$\Delta\delta$	$\langle x_\infty^* \rangle$	$\Delta x^*$
$1.0 \cdot 10^{-6}$	0.7099	$< 1.0 \cdot 10^{-4}$
$1.0 \cdot 10^{-5}$	0.7099	$< 1.0 \cdot 10^{-4}$
$1.0 \cdot 10^{-4}$	0.7101	$3.9 \cdot 10^{-3}$
$0.5 \cdot 10^{-3}$	0.7122	$1.9 \cdot 10^{-2}$
$1.0 \cdot 10^{-3}$	0.7162	$3.0 \cdot 10^{-2}$

that the average location of the transition layer does not change appreciably as long as  $\Delta\delta$  is of the same order as the average perturbation  $\delta_0$ . As  $\Delta\delta$  increases, the perturbation is no longer small compared with  $\delta_0$ , and the asymptotic results of § 3.1 do not necessarily apply. Indeed,  $\Delta x^*$  does not appear to vary linearly with  $\Delta\delta$ , as was the case in Table 6.

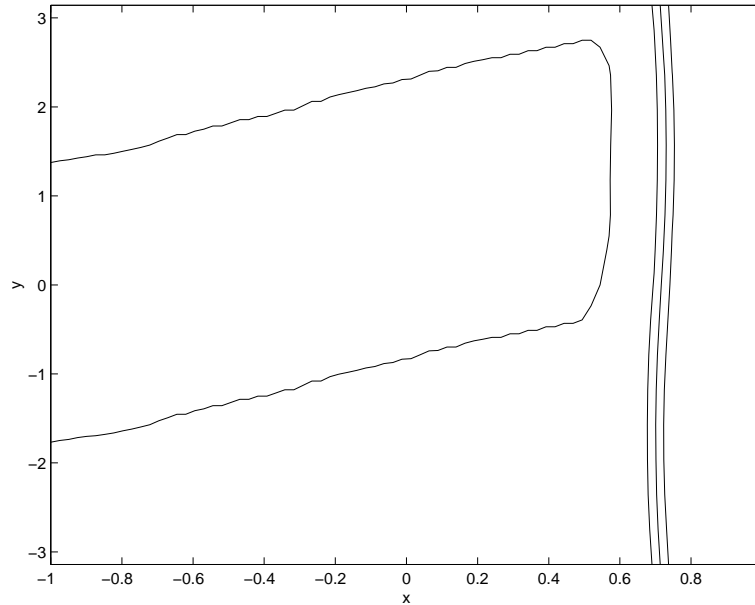
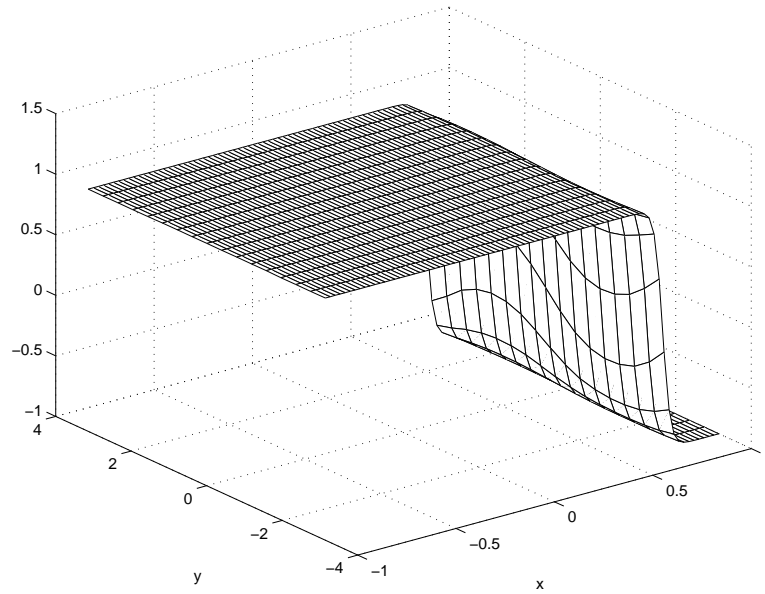
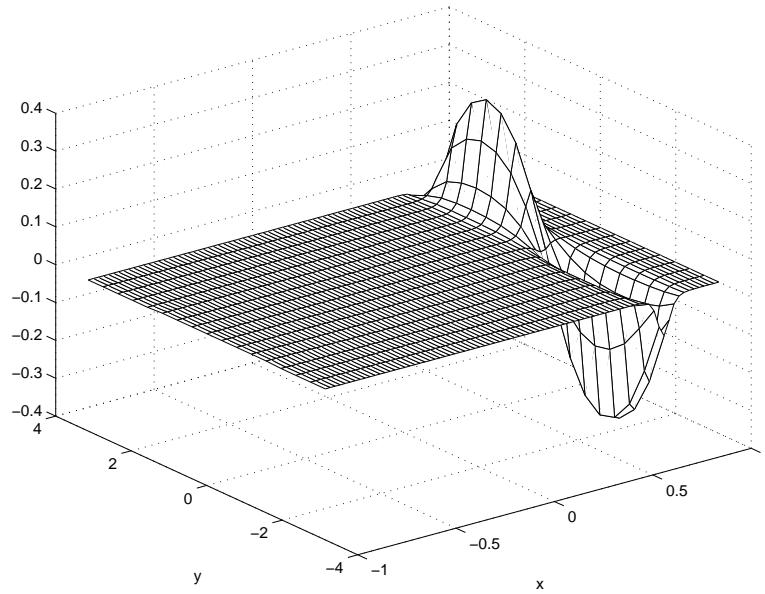


FIG. 2. Contour lines of the solution  $U$  at steady state.

A graphical representation of the computed solution  $U$  and its deviation from the profile function,  $U - u_0$ , for the case  $\Delta\delta = 1.0 \cdot 10^{-3}$  are given in Fig. 2 (contour lines of  $U$  at steady state) and Figs. 3 and 4 (perspective drawings of  $U$  and the difference

FIG. 3. *The solution  $U$  at steady state.*FIG. 4. *The difference  $U - u_0$  at steady state.*

$U - u_0$  at steady state). The data for these figures were taken after 2,500,000 time steps ( $\Delta t = 0.4$ ).

The results are quite good, but for long-time integration one would do better by looking for  $v$  in terms of its Fourier coefficients  $v_k$  and adopting an implicit scheme in the  $y$  direction. Thus, the constraint on the time step becomes the same as in the

one-dimensional case. The algorithm would be of the following type:

$$(48) \quad \varepsilon D_x^2 V_k^n + \frac{V_k^n - V_k^{n-1}}{\Delta t} + u_0 D_x V_k^n + (i\beta k u_0 + \varepsilon k^2) V_k^n + u_0' V^n = -\delta_0 \varepsilon^{-2} W_k^{n-1},$$

for  $n = 1, 2, \dots$ ;  $D_y$  is the matrix of differentiation with respect to  $y$  in Fourier space, and  $W_k$  is some approximation to the  $k$ th Fourier coefficient of  $vv_x + \beta vv_y$ .

This algorithm parallelizes with respect to the Fourier modes. It has been applied to a problem involving a propagating combustion front in a moving fluid [35, 36].

## REFERENCES

- [1] W. ECKHAUS, *Asymptotic Analysis of Singular Perturbations*, North-Holland, Amsterdam (1979).
- [2] D. R. SMITH, *Singular-Perturbation Theory*, Cambridge University Press (1985).
- [3] R. E. O'MALLEY, JR., *Singular Perturbation Methods for Ordinary Differential Equations*, Springer-Verlag, New York (1991).
- [4] J. KEVORKIAN AND J. D. COLE, *Multiple Scale and Singular Perturbation Problems*, Springer-Verlag, New York (1996).
- [5] E. M. DE JAGER AND JIANG FURU, *The Theory of Singular Perturbations*, Elsevier, Amsterdam (1996).
- [6] P. D. LAX, *Hyperbolic Systems of Conservation Laws and the Mathematical Theory of Shock Waves*, CBMS Regional Conference Series in Applied Mathematics, Vol. 11. SIAM, Philadelphia (1973).
- [7] K. TANUNA, *Asymptotic formulas for the shock wave of the scalar conservation law with smooth initial data*, Q. Appl. Math., **1** (1992) 109–128.
- [8] E. HOPF, *The partial differential equation  $u_t + uu_x = \mu u_{xx}$* , Comm. Pure Appl. Math. **3** (1950) 201–230.
- [9] P. C. FIFE, *Dynamics of Internal Layers and Diffusive Interfaces*, CBMS Regional Conference Series in Applied Mathematics, Vol. 53. SIAM, Philadelphia (1988).
- [10] J. LORENTZ, *Nonlinear singular perturbation problems and the Engquist-Osher difference scheme*, Report 8115, University of Nijmegen (1981).
- [11] G. KREISS AND H.-O. KREISS, *Convergence to steady state of solution of Burgers' equation*, Appl. Num. Math. **2** (1986) 161–179.
- [12] G. KREISS, *Convergence to steady state of solutions of viscous conservation laws*, in: *Asymptotic and Numerical Methods for Partial Differential Equations with Critical Parameters*, H. G. Kaper and M. Garbey (eds.), Kluwer Academic Publ., Dordrecht (1993), pp. 225–237.
- [13] J. G. L. LAFORGUE AND R. E. O'MALLEY, JR., *The supersensitivity of the shock layer location for Burgers' equation*, First Pan-American Workshop in Applied and Computational Mathematics (January, 1993).
- [14] J. G. L. LAFORGUE AND R. E. O'MALLEY, JR., *Supersensitive boundary value problems*, in: *Asymptotic and Numerical Methods for Partial Differential Equations with Critical Parameters*, H. G. Kaper and M. Garbey (eds.), Kluwer Academic Publ., Dordrecht (1993), pp. 215–224.
- [15] J. G. L. LAFORGUE AND R. E. O'MALLEY, JR., *On the motion of viscous shocks and the supersensitivity of their steady-state limits*, Meth. Appl. Anal. **1** (1994)
- [16] J. G. L. LAFORGUE AND R. E. O'MALLEY, JR., *Shock layer movement for Burgers' equation*, SIAM J. Appl. Math. **55** (1994)
- [17] J. G. L. LAFORGUE AND R. E. O'MALLEY, JR., *Viscous shock motion for advection-diffusion equations*, Studies in Applied Mathematics **95** (1995) 147–170.
- [18] J. G. L. LAFORGUE AND R. E. O'MALLEY, JR., *Exponential asymptotics, the viscous Burgers' equation, and standing wave solutions for a reaction-advection-diffusion model*, Studies in Applied Math., **102** (1999) 137–172.
- [19] L. G. REYNA AND M. J. WARD, *On the exponentially slow motion of a viscous shock*, Comm. Pure Appl. Math. **48** (1995) 79–120.
- [20] L. G. REYNA AND M. J. WARD, *On exponential ill-conditioning and internal layer behavior*, J. Num. Func. Analysis and Optimization **16** (1995) 475–500.
- [21] M. J. WARD AND L. G. REYNA, *Internal layers, small eigenvalues and the sensitivity of metastable motion*, SIAM J. Appl. Math. **55** (1995) 426–446.
- [22] J. D. BUCKMASTER AND G. S. S. LUDFORD, *Lectures on Mathematical Combustion*, CBMS Regional Conference Series in Applied Mathematics, Vol. 43. SIAM, Philadelphia (1983).

- [23] H.-G. ROOS, M. STYNES, AND L. TOBISKA, *Numerical Methods for Singularly Perturbed Differential Equations. Convection-diffusion and flow problems*. Springer Series in Computational Mathematics, Vol. 24, Springer-Verlag, Berlin (1996).
- [24] A. BAYLISS, D. GOTTLIEB, B. J. MATKOWSKY, AND M. MINKOFF, *An adaptive pseudo-spectral method for reaction diffusion problems*, J. Comp. Phys. **81** (1989) 421–443.
- [25] A. BAYLISS, T. BELYTSCHKO, D. HANSEN, AND E. TURKEL, *Adaptive multi-domain spectral methods*, in: *Proc. Fifth International Symposium on Domain Decomposition Methods for Partial Differential Equations (Norfolk, Virginia, 1991)*, T. F. Chan et al. (eds.), SIAM, Philadelphia (1992), pp. 195–203.
- [26] R. PEYRET, *The Chebyshev multidomain approach to stiff problems in fluid dynamics*, Comp. Meth. in Appl. Mech. and Engin. **80** (1990) 129–145.
- [27] M. GARBEY, *Domain decomposition to solve transition layers and asymptotic*, SIAM J. Sci. Comp. **15** (1994) 866–891.
- [28] M. GARBEY AND H. G. KAPER, *A heterogeneous domain decomposition method for singularly perturbed elliptic boundary value problems*, SIAM J. Num. Anal. **34** (1997), 1513–1544.
- [29] C. CANUTO, M. Y. HUSSAINI, A. QUARTERONI, AND T. A. ZANG, *Spectral Methods in Fluid Dynamics*, Springer-Verlag, New York (1988).
- [30] F. BREZZI, C. CANUTO, AND A. RUSSO, *A self-adaptive formulation for the Euler/ Navier-Stokes coupling*, Comput. Methods in Appl. Mech. and Eng. **73** (1989), 317–330.
- [31] R. ARINA AND C. CANUTO, *A self-adaptive domain decomposition for the viscous/ inviscid coupling. I. Burgers equation*, J. Comp. Phys. **105** (1993), 290–300.
- [32] Y. ACHDOU AND O. PIRONNEAU, *The  $\chi$ -method for the Navier-Stokes equation*, C. R. Acad. Sci. Paris **312** Série I (1991), 1005–1011.
- [33] L. ABRAHAMSSON AND S. OSHER, *Monotone difference schemes for singular perturbation problems*, SIAM J. Num. Anal. **19** (1982) 979–992.
- [34] F. DESPREZ AND M. GARBEY, *Direct numerical simulation of a combustion problem on the Paragon machine*, Parallel Computing **21** (1995), 495–508.
- [35] M. GARBEY AND D. TROMEUR-DERVOU, *Massively parallel computation of stiff propagating fronts*, Combustion Theory and Modeling **1** (1997), 271–294.
- [36] M. GARBEY AND D. TROMEUR-DERVOU, *A new parallel solver for the nonperiodic incompressible Navier-Stokes equations with a Fourier method: Application to frontal polymerization*, J. Comp. Phys. **145** (1998), 316–331.